

Simplifying Subgraph Representation Learning for Scalable Link Prediction

Paul Louis*, Shweta Ann Jacob and Amirali Salehi-Abari

Ontario Tech University, Canada

{paul.louis, shweta.jacob}@ontariotechu.net, abari@ontariotechu.ca

Abstract

Link prediction on graphs is a fundamental problem in graph representation learning. Subgraph representation learning approaches (SGRLs), by transforming link prediction to graph classification on the subgraphs around the target links, have advanced the learning capability of Graph Neural Networks (GNNs) for link prediction. Despite their state-of-the-art performance, SGRLs are computationally expensive, and not scalable to large-scale graphs due to their expensive subgraph-level operations for each target link. To unlock the scalability of SGRLs, we propose a new class of SGRLs, that we call *Scalable Simplified SGRL (S3GRL)*. Aimed at faster training and inference, *S3GRL* simplifies the message passing and aggregation operations in each link’s subgraph. *S3GRL*, as a scalability framework, flexibly accommodates various subgraph sampling strategies and diffusion operators to emulate computationally-expensive SGRLs. We further propose and empirically study multiple instances of *S3GRL*. Our extensive experiments demonstrate that the proposed *S3GRL* models scale up SGRLs without any significant performance compromise (even with considerable gains in some cases), while offering substantially lower computational footprints (e.g., multi-fold inference and training speedup).¹

1 Introduction

Graphs are ubiquitous in representing relationships between interacting entities in a variety of contexts, ranging from social networks [Chen *et al.*, 2020] to polypharmacy [Zitnik *et al.*, 2018]. One of the main tasks on graphs is link prediction [Liben-Nowell and Kleinberg, 2003], which involves predicting future or missing relationships between pairs of entities, given the structure of the graph. Link prediction plays a fundamental role in impactful areas, including molecular interaction prediction [Huang *et al.*, 2020], recommender systems

[Ying *et al.*, 2018], and protein-protein interaction prediction [Zhong *et al.*, 2022].

The early solutions to link prediction relied on hand-crafted, parameter-free heuristics based on the proximity of the source-target nodes [Page *et al.*, 1999; Adamic and Adar, 2003]. However, these methods require extensive domain knowledge for effective implementation. Recently, the success of *graph neural networks (GNNs)* in learning latent representations of nodes [Kipf and Welling, 2017] has led to their application in link prediction, through aggregating the source-target nodes’ representations as a link representation [Kipf and Welling, 2016; Pan *et al.*, 2018]. However, as GNNs learn a pair of nodes’ representations independent of their relative positions to each other, aggregating independent node representations results in poor link representations [Zhang *et al.*, 2021]. To circumvent this, the state-of-the-art subgraph representation learning approaches (SGRLs) [Zhang and Chen, 2018] learn enclosing subgraphs of pairs of source-target nodes, while augmenting node features with structural features.

The core issue hampering the deployment of GNNs and SGRLs is their high computational demands on large-scale graphs. Many approaches have been proposed for GNNs to relieve this bottleneck, ranging from sampling [Chen *et al.*, 2018; Zeng *et al.*, 2020] to simplification [Wu *et al.*, 2019] techniques. However, these techniques fail to be applied directly in SGRL models, where the issue is even more adverse due to subgraph extractions pertaining to each link. Although recent work has focused on tackling SGRL scalability by sampling [Yin *et al.*, 2022; Louis *et al.*, 2022] or sketching [Chamberlain *et al.*, 2022] approaches, little attention is given to simplification techniques. We focus on improving the scalability in SGRLs, by simplifying the underlying training mechanism.

Inspired by the simplification techniques in GNNs such as *SGCN* [Wu *et al.*, 2019] and *SIGN* [Frasca *et al.*, 2020], we propose *Scalable Simplified SGRL (S3GRL)* framework, which extends the simplification techniques to SGRLs. Our *S3GRL* is flexible in emulating many SGRLs by offering choices of subgraph sampling and diffusion operators, producing different-sized convolutional filters for each link’s subgraph. Our *S3GRL* benefits from precomputing the subgraph diffusion operators, leading to an overall reduction in runtimes while offering a multi-fold scale-up over existing

*Corresponding author.

¹Our code and experimental setup can be found online at <https://github.com/venomouslycyanide/S3GRL>.

SGRLs in training/inference times. We propose and empirically study multiple instances of our *S3GRL* framework. Our extensive experiments show substantial speedups in *S3GRL* models over state-of-the-art SGRLs while maintaining and sometimes surpassing their efficacies.

2 Related Work

Graph representation learning (GRL) [Hamilton, 2020] has numerous applications in drug discovery [Xiong *et al.*, 2019], knowledge graph completion [Zhang *et al.*, 2020], and recommender systems [Ying *et al.*, 2018]. The key downstream tasks in GRL are node classification [Hamilton *et al.*, 2017], link prediction [Zhang and Chen, 2018] and graph classification [Zhang *et al.*, 2018]. The early work in GRL, *shallow encoders* [Perozzi *et al.*, 2014; Grover and Leskovec, 2016], focused on learning dense latent node representations by taking multiple random walks rooted at each node. However, shallow encoders were incapable of consuming node features and being applied in the inductive settings. This shortcoming led to growing interest in Message Passing Graph Neural Networks (MPGNNs)² [Bruna *et al.*, 2014; Defferrard *et al.*, 2016] such as Graph Convolutional Networks (GCN) [Kipf and Welling, 2017]. In MPGNNs, node feature representations are iteratively updated by first aggregating neighborhood features and then updating them through non-linear transformations. MPGNNs differ in formulations of aggregation and update functions [Hamilton, 2020]. Link prediction is a fundamental problem on graphs, where the objective is to compute the likelihood of the presence of a link between a pair of nodes (e.g., users in a social network) [Liben-Nowell and Kleinberg, 2003]. Network heuristics such as Common Neighbors or Katz Index [Katz, 1953] were the first attempted solutions for link prediction. However, these predefined heuristics fail to generalize well on different graphs. To address this, MPGNNs have been used to learn representations of node pairs independently, then aggregate the representations for link probability prediction [Kipf and Welling, 2016; Mavromatis and Karypis, 2021]. However, this class of MPGNN solutions falls short in capturing graph automorphism and different structural roles of nodes in forming links [Zhang *et al.*, 2021]. SEAL [Zhang and Chen, 2018] successfully overcomes this limitation by casting the link prediction problem as a binary graph classification on the enclosing subgraph about a link, and adding structural labels to node features. This led to the emergence of subgraph representation learning approaches (SGRLs) [Zhang and Chen, 2018; Li *et al.*, 2020], which offer state-of-the-art results on the link prediction task. However, a common theme impeding the practicality and deployment of SGRLs is the lack of its scalability to large-scale graphs.

Recently, a new research direction has emerged in GNNs on scalable training and inference techniques, which mainly focuses on node classification tasks. A common practice is to use different sampling techniques—such as node sampling [Hamilton *et al.*, 2017], layer-wise sampling [Zou *et*

al., 2019], and graph sampling [Zeng *et al.*, 2020]—to subsample the training data to reduce computation. Other approaches utilize simplification techniques, such as removing intermediate non-linearities [Wu *et al.*, 2019; Frasca *et al.*, 2020], to speed up the training and inference. These approaches have been shown to fasten learning of MPGNNs (at the global level) for node and graph classification tasks, and even for link prediction [Pho and Mantzaris, 2022]; however, they are not directly applicable to SGRLs which exhibit superior performance for link prediction. In this work, we take the scalability-by-simplification approach for SGRLs (rather than for MPGNNs) by introducing *Scalable Simplified SGRL (S3GRL)*. Allowing diverse definitions of subgraphs and subgraph-level diffusion operators for SGRLs, *S3GRL* emulates SGRLs in generalization while speeding them up.

There is a growing interest in the scalability of SGRLs [Yin *et al.*, 2022; Louis *et al.*, 2022; Chamberlain *et al.*, 2022], with a main emphasis on the sampling approaches. SUREL [Yin *et al.*, 2022], by deploying random walks with restart, approximates subgraph structures; however, it does not use GNNs for link prediction. ScaL ed [Louis *et al.*, 2022] uses similar sampling techniques of SUREL, but to sparsify subgraphs in SGRLs for better scalability. ELPH/BUDDY [Chamberlain *et al.*, 2022] uses subgraph sketches as messages in MPGNNs but does not learn link representations explicitly at a subgraph level. Our work complements this body of research. Our framework can be combined with (or host) these methods for better scalability (see our experiments for an example).

3 Preliminaries

Consider an undirected graph $G = (V, E)$, where $V = \{1, \dots, n\}$ is the set of nodes (e.g., individuals, proteins), $E \subseteq V \times V$ represents their relationships (e.g., friendship or protein-to-protein interactions). We also let $\mathbf{A} \in \mathbb{R}^{n \times n}$ represent the *adjacency matrix* of G , where $A_{uv} > 0$ if and only if $(u, v) \in E$. We further assume each node possesses a d -dimensional feature vector (e.g., user’s profile, features of proteins, etc.) stored as a row in *feature matrix* $\mathbf{X} \in \mathbb{R}^{n \times d}$.

Link Prediction. The goal in link prediction is to infer the presence or absence of an edge between *target nodes* $T = \{u, v\}$ given the (partially) observed matrices \mathbf{A} and \mathbf{X} . The learning problem is to find a *likelihood function* f such that it assigns a higher likelihood to those target nodes with a missing link. The likelihood functions can be formulated by various neural network architectures, such as MLP [Guo *et al.*, 2022] and GNNs [Davidson *et al.*, 2018].

GNNs. Graph Neural Networks (GNNs) typically take as input \mathbf{A} and \mathbf{X} , apply L layers of convolution-like operations, and output $\mathbf{Z} \in \mathbb{R}^{n \times d'}$, containing d' -dimensional representation for each node as a row. For example, the l^{th} -layer output of Graph Convolution Network (GCN) [Kipf and Welling, 2017] is given by

$$\mathbf{H}^{(l)} = \sigma \left(\hat{\mathbf{A}} \mathbf{H}^{(l-1)} \mathbf{W}^{(l-1)} \right), \quad (1)$$

where *normalized adjacency matrix* $\hat{\mathbf{A}} = \tilde{\mathbf{D}}^{-\frac{1}{2}} \tilde{\mathbf{A}} \tilde{\mathbf{D}}^{-\frac{1}{2}}$, $\tilde{\mathbf{A}} = \mathbf{A} + \mathbf{I}$, $\tilde{\mathbf{D}}$ is the diagonal matrix with $\tilde{D}_{ii} = \sum_j \tilde{A}_{ij}$, and

²We use MPGNNs and GNNs interchangeably even though GNNs represent the broader class in GRL.

σ is a non-linearity function (e.g., ReLU). Here, $\mathbf{H}^{(0)} = \mathbf{X}$ and $\mathbf{W}^{(l)}$ is the l^{th} layer’s learnable weight matrix. After L stacked layers of Eq. 1, GCN outputs nodal-representation matrix $\mathbf{Z} = \mathbf{H}^{(L)}$. For any target nodes $T = \{u, v\}$, one can compute its joint representation:

$$\mathbf{q}_{uv} = \text{pool}(\mathbf{z}_u, \mathbf{z}_v), \quad (2)$$

where $\mathbf{z}_u, \mathbf{z}_v$ are u ’s and v ’s learned representations in \mathbf{Z} , and pool is a pooling/readout operation (e.g., Hadamard product or concatenation) to aggregate the pairs’ representations. Then, the link probability $p(u, v)$ for the target is given by $p(u, v) = \Omega(\mathbf{q}_{uv})$, where Ω is a learnable non-linear function (e.g., MLP) transforming the target embedding \mathbf{q}_{uv} into a link probability.

SGRL approaches (SGRLs). Subgraph representation learning approaches (SGRLs) [Zhang and Chen, 2017; Zhang and Chen, 2018; Zhang *et al.*, 2021; Yin *et al.*, 2022; Louis *et al.*, 2022] treat link prediction as a binary graph classification problem on enclosing subgraph $G_{uv} = (V_{uv} \subseteq V, E_{uv} \subseteq E)$ around a target $\{u, v\}$. SGRLs aim to classify if the enclosing subgraph G_{uv} is *closed* or *open* (i.e., the link exists or not). For each G_{uv} , SGRLs produce its nodal-representation matrix \mathbf{Z}_{uv} using the stack of convolution-like operators (see Eq. 1). Then, similar to Eq. 2, the nodal representations would be converted to link probabilities, with the distinction that the pooling function is graph pooling (e.g., SortPooling [Zhang *et al.*, 2018]), operating over all node’s representations (not just those of targets) to produce the fixed-size representation of the subgraph. To improve the expressiveness of GNNs on subgraphs, SGRLs augment node features with some structural features determined by the targets’ positions in the subgraph. These augmented features are known as *node labels* [Zhang *et al.*, 2021]. Node labeling techniques fall broadly into *identity (or zero-one)* or *geodesic distance-based* schemes [Huang *et al.*, 2022]. We refer to \mathbf{X}_{uv} as the matrix containing both the initial node features and labels generated by a valid labeling scheme [Zhang *et al.*, 2021]. The expressiveness power of SGRLs comes with high computational costs due to subgraph extractions, node labeling, and independent operations on overlapping large subgraphs. This computational overhead is exaggerated in denser graphs and deeper subgraphs due to the exponential growth of subgraph size.

SGCN and SIGN. To improve the scalability of GNNs for node classification tasks, several attempts are made to simplify GNNs by removing their intermediate nonlinearities, thus making them shallower, easier to train, and scalable. Simplified GCN (SGCN) [Wu *et al.*, 2019] has removed all but the last non-linearities in L -layer GCNs, to predict class label probabilities \mathbf{Y} for all nodes by

$$\mathbf{Y} = \xi(\hat{\mathbf{A}}^L \mathbf{X} \mathbf{W}), \quad (3)$$

where ξ is softmax or logistic function, and \mathbf{W} is the only learnable weight matrix. The term $\hat{\mathbf{A}}^L \mathbf{X}$ can be precomputed once before training. Benefiting from this precomputation and a shallower architecture, SGCN improves scalability. Recently, SIGN has extended SGCN to be more expressive yet scalable for node classification tasks. Its crux is to deploy a

set of linear diffusion matrices $\mathbf{M}^{(1)}, \dots, \mathbf{M}^{(r)}$ that can be applied to node-feature matrix \mathbf{X} . The class label probabilities \mathbf{Y} are computed by $\mathbf{Y} = \xi(\mathbf{Z} \mathbf{W}')$, where

$$\mathbf{Z} = \sigma \left(\bigoplus_{i=0}^r \mathbf{M}^{(i)} \mathbf{X} \mathbf{W}_i \right). \quad (4)$$

Here, ξ and σ are non-linearities, \mathbf{W}_i is the learnable weight matrix for diffusion operator $\mathbf{M}^{(i)}$, \bigoplus is a concatenation operation, and \mathbf{W}' is the learnable weight matrix for transforming node representations to class probabilities. Letting \mathbf{I} be the identity matrix, $\mathbf{M}^{(0)} = \mathbf{I}$ in Eq. 4 allows the node features to contribute directly (independent of graph structure) into the node representation and consequently to the class probabilities. The $\mathbf{M}^{(i)}$ operator can capture different heuristics in the graph. For example, the powers of the adjacency matrix as operators can capture the number of walks between nodes. Similar to SGCN, the terms $\mathbf{M}^{(i)} \mathbf{X}$ in SIGN can be once precomputed before training. These precomputations and the shallow architecture of SIGN lead to substantial speedup during training and inference with limited compromise on node classification efficacy. Motivated by these efficiencies, our proposed *S3GRL* framework extends SIGN for link prediction on subgraphs while addressing the computational bottleneck of SGRLs.

4 Scalable Simplified SGRL (S3GRL)

We propose *Scalable Simplified SGRL (S3GRL)*, which benefits from the expressiveness power of SGRLs while offering the simplicity and scalability of SIGN and SGCN for link prediction. Our framework leads to a multi-fold speedup in both training and inference of SGRL methods while maintaining or boosting their state-of-the-art performance (see experiments below).

Our *S3GRL* framework consists of two key components: (i) *Subgraph sampling strategy* $\Psi(G, T)$ takes as an input the graph G and target pairs $T = \{u, v\}$ and outputs the adjacency matrix \mathbf{A}_{uv} of the enclosing subgraphs G_{uv} around the targets. The subgraph sampling strategy Ψ can capture various subgraph definitions such as h -hop enclosing subgraphs [Zhang and Chen, 2018], random-walk-sampled subgraphs [Yin *et al.*, 2022; Louis *et al.*, 2022], and heuristic-based subgraphs [Zeng *et al.*, 2021]; (ii) *Diffusion operator* $\Phi(\mathbf{A}_{uv})$ takes the subgraph adjacency matrix \mathbf{A}_{uv} and outputs its diffusion matrix \mathbf{M}_{uv} . A different class of diffusion operators are available: adjacency/Laplacian operators to capture connectivity, triangle/motif-based operators [Granovetter, 1983] to capture inherent community structure, personalized pagerank-based (PPR) operators [Gasteiger *et al.*, 2019] to identify important connections. Each of these operators and their powers can constitute the different diffusion operators in *S3GRL*.

In our *S3GRL* framework, each model is characterized by the *sampling-operator* set $\mathcal{S} = \{(\Psi_i, \Phi_i)\}_{i=0}^r$, where Ψ_i and Φ_i are the i^{th} subgraph sampling strategy and diffusion operator, respectively. For a graph G , target pair $T = \{u, v\}$, and sampling-operator pair (Ψ_i, Φ_i) , one can find T ’s sampled subgraph $\mathbf{A}_{uv}^{(i)} = \Psi_i(G, T)$ and its corresponding diffusion

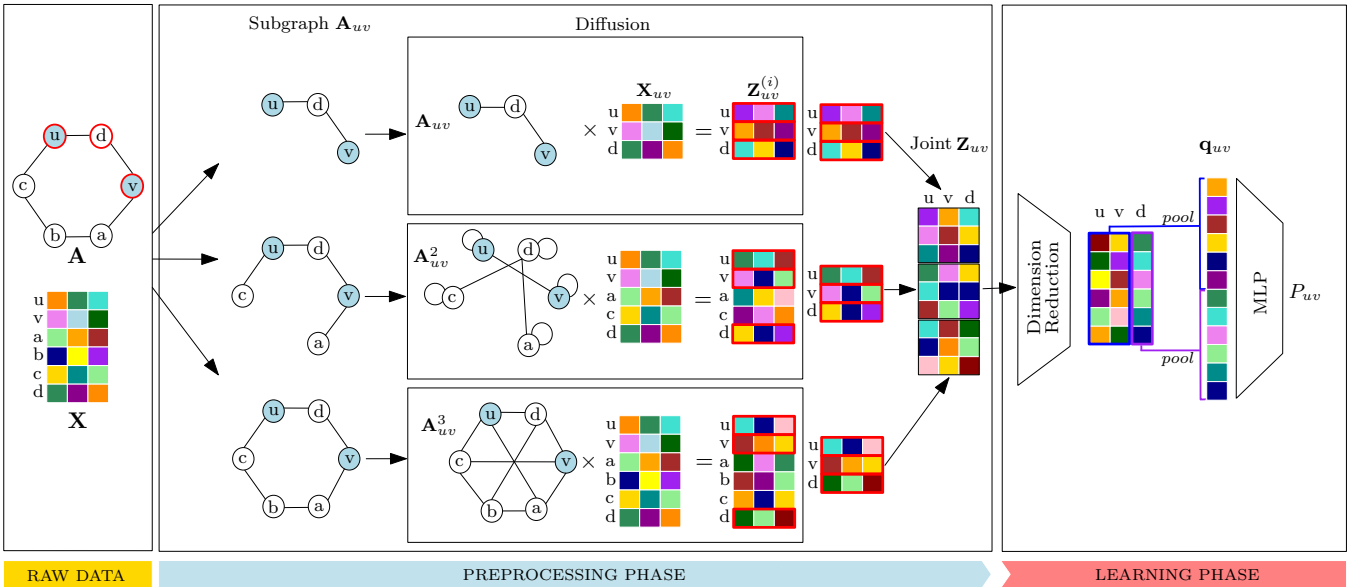


Figure 1: Our *S3GRL* framework: In the preprocessing phase (shown by the shaded blue arrow), first multiple subgraphs are extracted around the target nodes u and v (shaded in blue) by various sampling strategies. Diffusion matrices are then created from extracted subgraph adjacency matrices by predefined diffusion operators (e.g., powers of subgraphs in this figure). Each diffusion process involves the application of the subgraph diffusion matrix on its nodal features to create the matrix $\mathbf{Z}_{uv}^{(i)}$. The operator-level node representations of selected nodes (with a red border in raw data) are then aggregated for all subgraphs to form the joint \mathbf{Z}_{uv} matrix. The selected nodes in this example are the target nodes $\{u, v\}$, and their common neighbor d . In the learning phase (as shown by the shaded red arrow), the joint matrix \mathbf{Z}_{uv} undergoes dimensionality reduction followed by pooling using center pooling (highlighted by blue-border box) and common neighbor pooling (highlighted by purple-border box). Finally, the target representation \mathbf{q}_{uv} is transformed by an MLP to a link probability P_{uv} .

matrix $\mathbf{M}_{uv}^{(i)} = \Phi_i(\mathbf{A}_{uv}^{(i)})$. For instance, one can define Ψ_i to sample the random-walk-induced subgraph $\mathbf{A}_{uv}^{(i)}$ rooted at $\{u, v\}$ in G . Then, Φ_i can compute the l -th power of $\mathbf{A}_{uv}^{(i)}$, to count the number of l -length walks on the subgraph. *S3GRL* computes the operator-level node representations of the selected subgraph $\mathbf{A}_{uv}^{(i)}$ by

$$\mathbf{Z}_{uv}^{(i)} = \mathbf{M}_{uv}^{(i)} \mathbf{X}_{uv}^{(i)}. \quad (5)$$

Here, $\mathbf{X}_{uv}^{(i)}$ is the node feature matrix for nodes in the selected subgraph $\mathbf{A}_{uv}^{(i)}$ for the sampling-operator pair (Ψ_i, Φ_i) . Eq. 5 can be viewed as feature smoothing where the diffusion matrix $\mathbf{M}_{uv}^{(i)}$ is applied over node features $\mathbf{X}_{uv}^{(i)}$. *S3GRL* then concatenates the operator-level nodal-representation matrix $\mathbf{Z}_{uv}^{(i)}$ of all sampling-operator pairs to form the *joint nodal-representation matrix*:

$$\mathbf{Z}_{uv} = \bigoplus_{i=0}^r \mathbf{Z}_{uv}^{(i)} \quad (6)$$

The concatenation between nodal-representation matrices with dimensionality mismatch should be done with care: the corresponding rows (belonging to the same node) should be inline, where missing rows are filled with zeros (analogous to zero-padding for graph pooling). The joint nodal-representation matrix \mathbf{Z}_{uv} goes through a non-linear feature transformation (for dimensionality reduction) by learnable weight matrix \mathbf{W} and non-linearity σ . This transformed matrix is then further downsampled by the graph pooling pool to form the target's representation:

$$\mathbf{q}_{uv} = \text{pool}(\sigma(\mathbf{Z}_{uv} \mathbf{W})), \quad (7)$$

from which the link probability is computed by

$$P_{uv} = \Omega(\mathbf{q}_{uv}), \quad (8)$$

with Ω being a learnable non-linear function (e.g., MLP) to convert the target representation \mathbf{q}_{uv} into a link probability.

Our *S3GRL* exhibits substantial speedup in inference and training through precomputing \mathbf{Z}_{uv} in comparison to more computationally-intensive SGRLs [Li *et al.*, 2020; Pan *et al.*, 2022], designed based on multi-layered GCN or DGCNN [Zhang *et al.*, 2018] (see our experiments for details). Note that only Equations 7 and 8 are utilized in training and inference in *S3GRL* (see also Figure 1). Apart from this computational speedup, *S3GRL* offers other advantages analogous to other prominent GNNs:

Disentanglement of Data and Model. The composition of subgraph sampling strategy Ψ and diffusion operator Φ facilitates the disentanglement (or decoupling) of data (i.e., subgraph) and model (i.e., diffusion operator). This disentanglement resembles shaDow-GNN [Zeng *et al.*, 2021], in which the depth of GNNs (i.e., its number of layers) is decoupled from the depth of enclosing subgraphs. Similarly, in *S3GRL*, one can explore high-order diffusion operators (e.g., adjacency matrix to a high power) in constrained enclosing subgraphs (e.g., ego network of the target pair). This combination simulates multiple message-passing updates between the nodes in the local subgraph, thus achieving local oversmoothing [Zeng *et al.*, 2021] and ensuring the final subgraph representation possesses information from all the nodes in the local subgraph.

Multi-View Representation. Our *S3GRL* framework via the sampling-operator pairs provides multiple views of the enclosing neighborhood of each target pair. This capability allows hosting models analogous to multi-view [Abu-El-Haija *et al.*, 2020; Cai and Ji, 2020] models.

5 *S3GRL* Instances: PoS and SoP

We introduce two instances of *S3GRL*, differentiating in the choice of sampling-operator pairs.

Powers of Subgraphs (PoS). This instance intends to mimic a group of SGRLs with various model depths on a fixed-sized enclosing subgraph while boosting scalability and generalization (e.g., SEAL [Zhang and Chen, 2018]). The sampling-operator set $\mathcal{S} = \{(\Psi_i, \Phi_i)\}_{i=0}^r$ is defined as follows: (i) the sampling strategy $\Psi_i(G, T)$ for any i is constant and returns the adjacency matrix \mathbf{A}_{uv} of the h -hop enclosing subgraph G_{uv}^h about target $T = \{u, v\}$. The subgraph G_{uv}^h is a node-induced subgraph of G with the node set $V_{uv}^h = \{j | d(j, u) \leq h \text{ or } d(j, v) \leq h\}$, including the nodes with the geodesic distance of at most h from either of the target pairs [Zhang and Chen, 2018]; (ii) the i -th diffusion operator $\Phi_i(\mathbf{A}) = \mathbf{A}^i$ is the i -th power of adjacency matrix \mathbf{A} . This operator facilitates information diffusion among nodes i -length paths apart. Putting (i) and (ii) together, one can derive $\mathbf{M}_{uv}^{(i)} = \mathbf{A}_{uv}^i$ for Eq. 5. Note that $\mathbf{M}_{uv}^{(0)} = \mathbf{I}$ allows the node features to contribute directly (independent of graph structure) to subgraph representation. PoS possesses two hyperparameters r and h , controlling the number of diffusion operators and the number of hops in enclosing subgraphs, respectively.

One can intuitively view PoS as equivalent to SEAL that uses a GNN model of depth r with “skip-connections” [Xu *et al.*, 2018] on the h -hop enclosing subgraphs. The skip-connections property allows consuming all the intermediate learned representations of each layer to construct the final link representation. Similarly, PoS uses varying i -th power diffusion operators combined with the concatenation operator in Eq. 7 to generate the representation \mathbf{q}_{uv} . In this light, the two hyperparameters of r and h (resp.) in PoS control the (virtual) depth of the model and the number of hops in enclosing subgraphs (resp.).

Subgraphs of Powers (SoP). This instance of *S3GRL*, by transforming the global input graph G , brings long-range interactions into the local enclosing subgraphs. Let $\Psi_H(G, T, h)$ be h -hop sampling strategy, returning the enclosing h -hop subgraph about the target pair $T = \{u, v\}$. The SoP model defines $\mathcal{S} = \{(\Psi_i, \Phi_i)\}_{i=0}^r$ with $\Psi_i(G, T) = \Psi_H(G^i, T, h)$ and $\Phi_i(\mathbf{A}_{uv}) = \mathbf{A}_{uv}$. Here, G^i is the i -th power of the input graph (computed by \mathbf{A}^i), in which two nodes are adjacent when their geodesic distance in G is at most i . In this sense, the power of graphs brings long-range interactions to local neighborhoods at the cost of neighborhood densification. However, as the diffusion operator is an identity function, SoP prevents overarching to the further-away information of indirect neighbors. SoP consists of two hyperparameters r and h that control the number of diffusion operators and hops in local subgraphs, respectively.

PoS vs. SoP. PoS and SoP are similar in capturing informa-

tion diffusion among nodes (at most) r -hop apart. But, their key distinction is whether long-range diffusion occurs in the global level of the input graph (for SoP) or the local level of the subgraph (for PoS). SoP does not fall into the category of “typical” SGRLs, however, it still uses subgraphs around the target pair on the power of graphs.

Graph Pooling. Our proposed instances of *S3GRL* are completed by defining the graph pooling function in Eq. 7. We specifically consider computationally-light pooling functions, which focus on pooling the targets’ or their direct neighbors’ learned representations.³ We consider simple *center* pooling: $\text{pool}_C(\mathbf{Z}) = \mathbf{z}_u \odot \mathbf{z}_v$, where \odot is the Hadamard product, and $\mathbf{z}_u, \mathbf{z}_v$ are u ’s and v ’s learned representations in nodal-representation matrix \mathbf{Z} (i.e., the two rows of the target pairs in \mathbf{Z}). We also introduce *common-neighbor* pooling: $\text{pool}_N(\mathbf{Z}) = \text{AGG}(\{\mathbf{z}_i | i \in N_u \cap N_v\})$, where AGG is any invariant graph readout function (e.g., mean, max, or sum), and N_u and N_v are the direct neighborhood of targets u, v in the original input graph. We also define *center-common-neighbor* pooling $\text{pool}_{CCN} = \text{pool}_C \oplus \text{pool}_N$. In addition to their efficacy, these pooling functions allow one to further optimize the data storage and computations. As the locations of *pooled nodes* (e.g., target pairs and/or their direct neighbors) for these pooling functions are specified in the original graph, one could just conduct necessary (pre)computations and store those data affecting the learned representation of pooled nodes, while avoiding unnecessary computations and data storage. Figure 1 shows this optimization through red-bordered boxes of rows for each $\mathbf{Z}_{uv}^{(i)}$. This information is the only required node representations in $\mathbf{Z}_{uv}^{(i)}$ utilized in the downstream pool operation. We consider center pooling as the default pooling for PoS and SoP, and we refer to them as PoS⁺ and SoP⁺ when center-common-neighbor pooling is deployed.

Inference Time Complexity. Let p be the number of pooled nodes (e.g., $p = 2$ for center pooling), d be the dimension of initial input features, r be the number of operators, and d' be the reduced dimensionality in Eq. 7. The inference time complexity for any of PoS, SoP, and their variants is $O(rpdd' + d'^2)$. Consider the dimensionality reduction of the joint matrix \mathbf{Z}_{uv} by the weight matrix \mathbf{W} in Eq. 7. As \mathbf{Z}_{uv} is rp by d and \mathbf{W} is d by d' , their multiplication is in $O(rpdd')$ time. The pooling for any proposed variants is $O(pd')$. Assuming Ω in Eq. 8 being an MLP with one d' -dimensional hidden layer, its computation is in $O(d'^2)$ time.

6 Experiments

We carefully design a set of extensive experiments to assess the extent to which our model scales up SGRLs while maintaining their state-of-the-art performance. Our experiments intend to address these questions: **(Q1)** How effective is the *S3GRL* framework compared with the state-of-the-art link prediction methods (e.g., SGRLs)? **(Q2)** What is the

³Our focus is backed up by recent empirical findings [Chamberlain *et al.*, 2022] showing the effectiveness of the target node’s embeddings and the decline in the informativeness of node embeddings as the nodes get farther away from targets.

	Dataset	# Nodes	# Edges	Avg. Deg.	# features
Non-Attributed	NS	1461	2742	3.75	NA
	Power	4941	6594	2.67	NA
	Yeast	2375	11693	9.85	NA
	PB	1222	16714	27.36	NA
Attributed	Cora	2708	4488	3.31	1433
	CiteSeer	3327	3870	2.33	3703
	PubMed	19717	37676	3.82	500
	Texas	183	143	1.56	1703
	Wisconsin	251	197	1.57	1703

Table 1: The statistics of the non-attributed and attributed datasets.

computational gain achieved through *S3GRL* in comparison to SGRLs? (Q3) How complementary can *S3GRL* be in combination with other scalable SGRLs (e.g., ScaL ed [Louis *et al.*, 2022]) to further boost scalability and generalization?

Dataset. For our experiments, we use homogeneous, undirected, attributed and non-attributed datasets that are publicly available and commonly used in other link prediction studies [Zhang and Chen, 2018; Zhang *et al.*, 2018; Li *et al.*, 2020; Pan *et al.*, 2022; Louis *et al.*, 2022]. Table 1 shows the statistics of our datasets. The edges in each dataset are randomly split into 85% training, 5% validation, and 10% testing sets.

Baselines. We compare our *S3GRL* models (PoS, PoS⁺, and SoP) with 15 baselines belonging to five different categories of link prediction models. Our *heuristic* benchmarks include common neighbors (CN), Adamic Adar (AA), and personalized pagerank (PPR). For *message-passing GNNs* (MPGNNs), we select GCN [Kipf and Welling, 2017], GraphSAGE [Hamilton *et al.*, 2017] and GAT [Vaswani *et al.*, 2017]. Our *latent factor* (LF) benchmarks are node2vec [Grover and Leskovec, 2016] and Matrix Factorization [Koren *et al.*, 2009]. The *autoencoder* (AE) methods include GAE & VGAE [Kipf and Welling, 2016], adversarially regularized variational graph autoencoder (ARVGA) [Pan *et al.*, 2018] and Graph InfoClust (GIC) [Mavromatis and Karypis, 2021]. Finally, our examined SGRLs include SEAL [Zhang and Chen, 2018], GCN+DE (distance encoding [Li *et al.*, 2020])⁴, and the state-of-the-art WalkPool [Pan *et al.*, 2022].⁵

Setup. For SGRL and *S3GRL* methods, we set the number of hops $h = 2$ for the non-attributed datasets (except WalkPool on the Power dataset with $h = 3$) and $h = 3$ on attributed datasets (except for WalkPool with $h = 2$ based on [Pan *et al.*, 2022]).⁶ In *S3GRL* models, we set the number of operators $r = 3$, and use zero-one labeling scheme. The *AGG* graph readout function in center-common-neighbor pooling is set to a simple mean aggregation. In *S3GRL* models, across all datasets, we set the hidden dimension in Eq. 7 to 256, and also implement Ω in Eq. 8 as an MLP with one 256-dimensional

⁴We replicate DE-GNN [Li *et al.*, 2020] using SEAL-OGB code [Zhang *et al.*, 2021]. This code uses a GCN with the distance encoding labeling trick.

⁵We postpone an empirical comparison to ELPH/BUDDY [Chamberlain *et al.*, 2022] as its code is not released, probably due to being under review; see Section 2 for how *S3GRL* differentiates.

⁶All hyperparameters of baselines are optimally selected based on their original papers or the shared public implementations. When possible, we also select the *S3GRL* hyperparameters to match the benchmarks’ hyperparameters for a fair comparison.

hidden layer. For all models, we set the dropout to 0.5 and train them for 50 epochs with Adam [Kingma and Ba, 2015] and a batch size of 32 (except for MPGNNs with full-batch training on the input graph). See the Appendix for additional details on the experimental setup.

For all models, we report the average of the area under the curve (AUC) of the testing data over 10 runs with different fixed random seeds.⁷ In each run, we test a model on the testing data with those parameters with the highest AUC on the validation data. Our code is implemented in PyTorch Geometric [Fey and Lenssen, 2019] and PyTorch [Paszke *et al.*, 2019].⁸ To compare the computational efficiency, we report the average training and inference time (over 50 epochs) and the total preprocessing and runtime for a fixed run.

Results. Table 2 shows the AUC results for all models and datasets. Also, the resource consumption comparisons between competitive SGRLs vs *S3GRL* models are in Table 3.

On the attributed datasets, the *S3GRL* models, particularly PoS⁺ and PoS, consistently outperform others (see Table 2). Their gain/improvement, compared to the best baseline, can reach 2.93 (for Wisconsin) and 2.77 (for CiteSeer). This state-of-the-art performance of PoS⁺ and PoS suggests that our simplification techniques do not weaken SGRLs’ efficacy and even improves their generalizability. Most importantly, this AUC gain is achieved by multi-fold less computation: The *S3GRL* models benefit 2.3–13.8x speedup in training time for citation network datasets of Cora, CiteSeer, and Pubmed (see Table 3). Similarly, inference time witnesses 3.1–51.2x speedup, where the maximum speedup is achieved on the largest attributed dataset Pubmed. Our *S3GRL* models exhibit higher dataset preprocessing times compared to SGRLs (see Table 3). However, this is easily negated by our models’ faster accumulative training and inference times that lead to 1.4–11.9x overall runtime speedup across all attributed datasets (min. for Texas and max. for Pubmed).

We observe comparatively lower AUC values for SoP, which can be attributed to longer-range information being of less value on these datasets. Regardless, SoP still shows comparable AUC to the other SGRLs while offering substantially higher speedups.

Despite only consuming the source-target information, PoS achieves first or second place in the citation networks indicating the power of the center pooling. Moreover, the higher efficacy of PoS⁺ compared to PoS across a few datasets indicate added expressiveness provided by center-common-neighbor pooling. Finally, the autoencoder methods outperform SGRLs on citation networks. However, *S3GRL* instances outperform them and have enhanced the learning capability of SGRLs.

For the non-attributed datasets, although WalkPool outperforms others, we see strong performance from our *S3GRL* instances. Our instances appear second or third (e.g., Yeast or Power) or have a small margin to the best model (e.g., NS or PB). The maximum loss in our models is bounded to

⁷We exclude Average Precision (AP) results due to their known strong correlations with AUC results [Pan *et al.*, 2022].

⁸All experiments are run on servers with 50 CPU cores, 377 GB RAM, and 11 GB GTX 1080 Ti GPUs.

	Model	Non-attributed				Attributed				
		NS	Power	PB	Yeast	Cora	CiteSeer	PubMed	Texas	Wisconsin
Heuristic	AA	92.14 ± 0.77	58.09 ± 0.55	91.76 ± 0.56	88.80 ± 0.55	71.48 ± 0.69	65.86 ± 0.80	64.26 ± 0.40	54.69 ± 3.68	55.60 ± 3.14
	CN	92.12 ± 0.79	58.09 ± 0.55	91.44 ± 0.59	88.73 ± 0.56	71.40 ± 0.69	65.84 ± 0.81	64.26 ± 0.40	54.36 ± 3.65	55.08 ± 3.08
	PPR	92.50 ± 1.06	62.88 ± 2.18	86.85 ± 0.48	91.71 ± 0.74	82.87 ± 1.01	74.35 ± 1.51	75.80 ± 0.35	53.81 ± 7.53	62.86 ± 8.13
MPGNN	GCN	91.75 ± 1.68	69.41 ± 0.90	90.80 ± 0.43	91.29 ± 1.11	89.14 ± 1.20	87.89 ± 1.48	92.72 ± 0.64	67.42 ± 9.39	72.77 ± 6.96
	GraphSage	91.39 ± 1.73	64.94 ± 2.10	88.47 ± 2.56	87.41 ± 1.64	85.96 ± 2.04	84.05 ± 1.72	81.60 ± 1.22	53.59 ± 9.37	61.81 ± 9.66
	GIN	83.26 ± 3.81	58.28 ± 2.61	88.42 ± 2.09	84.00 ± 1.94	68.74 ± 2.74	69.63 ± 2.77	82.49 ± 2.89	63.46 ± 8.87	70.82 ± 8.25
LF	node2vec	91.44 ± 0.81	73.02 ± 1.32	85.08 ± 0.74	90.60 ± 0.57	78.32 ± 0.74	75.36 ± 1.22	79.98 ± 0.35	52.81 ± 5.31	59.57 ± 5.69
	MF	82.56 ± 5.90	53.83 ± 1.76	91.56 ± 0.56	87.57 ± 1.64	62.25 ± 2.21	61.65 ± 3.80	68.56 ± 12.13	60.35 ± 5.62	53.75 ± 9.00
AE	GAE	92.50 ± 1.71	68.17 ± 1.64	91.52 ± 0.35	93.13 ± 0.79	90.21 ± 0.98	88.42 ± 1.13	94.53 ± 0.69	68.67 ± 6.95	75.10 ± 8.69
	VGAE	91.83 ± 1.49	66.23 ± 0.94	91.19 ± 0.85	90.19 ± 1.38	92.17 ± 0.72	90.24 ± 1.10	92.14 ± 0.19	74.61 ± 8.61	74.39 ± 8.39
	ARVGA	92.16 ± 1.05	66.26 ± 1.59	90.98 ± 0.92	90.25 ± 1.06	92.26 ± 0.74	90.29 ± 1.01	92.10 ± 0.38	73.55 ± 9.01	72.65 ± 7.02
	GIC	90.88 ± 1.85	62.01 ± 1.25	73.65 ± 1.36	88.78 ± 0.63	91.42 ± 1.24	92.99 ± 1.14	91.04 ± 0.61	65.16 ± 7.87	75.24 ± 8.45
SGRL	SEAL	98.63 ± 0.67	85.28 ± 0.91	95.07 ± 0.35	97.56 ± 0.32	90.29 ± 1.89	88.12 ± 0.85	97.82 ± 0.28	71.68 ± 6.85	77.96 ± 10.37
	GCN+DE	98.66 ± 0.66	80.65 ± 1.40	95.14 ± 0.35	96.75 ± 0.41	91.51 ± 1.10	88.88 ± 1.53	98.15 ± 0.11	76.60 ± 6.40	74.65 ± 9.56
	WalkPool	98.92 ± 0.52	90.25 ± 0.64	95.50 ± 0.26	98.16 ± 0.20	92.24 ± 0.65	89.97 ± 1.01	98.36 ± 0.11	78.44 ± 9.83	79.57 ± 11.02
S3GRL	PoS (ours)	97.23 ± 1.38	86.67 ± 0.98	94.83 ± 0.41	95.47 ± 0.54	94.65 ± 0.67	95.76 ± 0.59	98.97 ± 0.08	73.75 ± 8.20	82.50 ± 5.83
	PoS+ (ours)	98.37 ± 1.26	87.82 ± 0.96	95.04 ± 0.27	96.77 ± 0.39	94.77 ± 0.68	95.72 ± 0.56	99.00 ± 0.08	78.44 ± 9.83	79.17 ± 10.87
	SoP (ours)	90.61 ± 1.94	75.64 ± 1.33	94.34 ± 0.30	92.98 ± 0.58	91.24 ± 0.80	88.23 ± 0.73	95.91 ± 0.29	69.49 ± 7.12	72.29 ± 14.42
	Gain	-0.55	-2.43	-0.46	-1.39	+2.51	+2.77	+0.64	0	+2.93

Table 2: Average AUC for attributed and non-attributed datasets (over 10 runs). The top 3 models are indicated by **First**, **Second**, and **Third**. **Green** is best model among our *S3GRL* variants. **Yellow** is the best baseline. Gain is AUC difference of **Green** and **Yellow**.

Model	Training	Inference	Preproc.	Runtime	Training	Inference	Preproc.	Runtime	Training	Inference	Preproc.	Runtime
	NS (non-attributed)				Power (non-attributed)				Yeast (non-attributed)			
SEAL	4.91 ± 0.23	0.14 ± 0.01	17.86	275.28	11.73 ± 0.02	0.33 ± 0.01	44.48	658.14	24.03 ± 0.40	0.54 ± 0.05	115.02	1362.85
GCN+DE	3.58 ± 0.12	0.10 ± 0.01	11.73	198.98	8.62 ± 0.27	0.25 ± 0.01	28.59	479.4	18.41 ± 0.71	0.46 ± 0.06	82.19	1040.72
WalkPool	7.66 ± 0.09	0.41 ± 0.02	12.18	427.03	18.46 ± 0.76	0.87 ± 0.06	33.51	1024.55	174.80 ± 1.06	8.05 ± 0.11	90.75	9443.17
PoS	2.24 ± 0.15	0.06 ± 0.01	34.86	152.23	5.58 ± 0.48	0.14 ± 0.01	97.71	388.97	9.95 ± 1.45	0.20 ± 0.06	259.96	775.58
PoS+	2.54 ± 0.06	0.07 ± 0.00	41.43	173.78	6.12 ± 0.24	0.16 ± 0.01	107.77	426.53	10.49 ± 0.61	0.20 ± 0.04	206.52	749.87
SoP	2.26 ± 0.11	0.06 ± 0.00	24.67	142.45	5.41 ± 0.23	0.14 ± 0.01	65.65	347.62	9.24 ± 0.74	0.22 ± 0.04	117.23	597.29
Speedup	3.42(1.41)	6.83(1.43)	0.72(0.28)	3.00(1.14)	3.41(1.41)	6.21(1.56)	0.68(0.27)	2.95(1.12)	18.92(1.76)	40.25(2.09)	0.98(0.32)	15.81(1.34)
	PB (non-attributed)				Cora (attributed)				CiteSeer (attributed)			
SEAL	64.62 ± 5.59	2.32 ± 0.10	531.79	3947.45	18.37 ± 1.49	0.73 ± 0.12	113.32	1090.94	12.54 ± 0.69	0.58 ± 0.10	93.52	768.72
GCN+DE	55.82 ± 1.59	2.01 ± 0.09	398.81	3346.80	14.85 ± 0.53	0.62 ± 0.08	80.48	872.68	11.43 ± 0.71	0.52 ± 0.07	71.97	685.98
WalkPool	133.30 ± 0.52	6.48 ± 0.15	136.29	7291.50	18.53 ± 0.91	1.00 ± 0.15	27.43	1034.33	15.32 ± 0.54	0.87 ± 0.05	22.82	859.27
PoS	13.42 ± 0.77	0.33 ± 0.04	1754.88	2452.39	5.44 ± 0.52	0.15 ± 0.02	106.45	394.12	4.82 ± 0.22	0.15 ± 0.01	78.62	335.37
PoS+	15.56 ± 1.28	0.29 ± 0.05	2527.23	3331.56	5.87 ± 0.17	0.17 ± 0.01	93.69	401.05	4.91 ± 0.39	0.17 ± 0.02	72.02	331.55
SoP	13.32 ± 0.72	0.25 ± 0.06	333.58	1022.90	5.04 ± 0.17	0.15 ± 0.03	35.65	300.10	4.96 ± 0.14	0.17 ± 0.01	31.57	293.96
Speedup	10.01(3.59)	25.92(6.09)	1.59(0.05)	7.13(1.00)	3.68(2.53)	6.67(3.65)	3.18(0.26)	3.64(2.18)	3.18(2.30)	5.80(3.06)	2.96(0.29)	2.92(2.05)
	PubMed (attributed)				Texas (attributed)				Wisconsin (attributed)			
SEAL	533.18 ± 4.64	38.46 ± 1.08	141.76	30150.31	0.32 ± 0.01	0.01 ± 0.00	2.55	20.46	0.47 ± 0.01	0.02 ± 0.00	3.29	29.27
GCN+DE	423.73 ± 2.67	34.44 ± 1.21	106.00	24311.00	0.31 ± 0.01	0.01 ± 0.00	1.87	18.55	0.43 ± 0.01	0.02 ± 0.00	2.63	26.19
WalkPool	150.27 ± 6.22	8.10 ± 1.06	341.12	8474.72	0.55 ± 0.08	0.03 ± 0.01	0.92	32.54	0.85 ± 0.04	0.06 ± 0.00	1.08	49.38
PoS	38.90 ± 2.89	0.79 ± 0.10	2986.74	5017.78	0.16 ± 0.01	0.01 ± 0.00	1.87	12.71	0.21 ± 0.02	0.01 ± 0.00	2.65	15.86
PoS+	45.32 ± 2.21	0.92 ± 0.11	2976.80	5335.86	0.18 ± 0.01	0.01 ± 0.00	2.26	11.96	0.24 ± 0.02	0.01 ± 0.00	2.91	16.07
SoP	38.38 ± 2.90	0.75 ± 0.15	526.62	2526.22	0.15 ± 0.01	0.01 ± 0.00	1.34	9.61	0.22 ± 0.01	0.01 ± 0.00	1.87	13.75
Speedup	13.89(3.32)	51.28(8.80)	0.65(0.04)	11.93(1.59)	2.62(1.72)	3.00(1.00)	1.90(0.41)	3.39(1.46)	4.05(1.79)	6.00(2.00)	1.76(0.37)	3.59(1.63)

Table 3: Computation time of SGRLs vs. our *S3GRL* models: average training time (over 50 epochs), average inference time, preprocessing time, and total runtime (preprocessing, training, and inference time) for 50 epochs. **Green** is the fastest and **Red** is slowest for each group of SGRLs and *S3GRL*. Max(min) speedup corresponds to the ratio of time taken by the slowest (fastest) SGRLs to our fastest (slowest) model.

2.43% (see Power’s gain in Table 2). Regardless of the small loss of efficacy, our *S3GRL* models demonstrate multi-fold speedup in training and inference times: training with 1.4–18.9x speedup and inference with 1.4–40.2x (the maximum training and inference speedup on Yeast). We see a similar pattern of higher preprocessing times for our models; however, it gets negated by faster training and inference times leading to an overall speedup in runtimes with the maximum of 15.8x for Yeast. SoP shows a relatively lower AUC in the

non-attributed dataset except for PB and Yeast, possibly indicating that long-range information is more crucial for them.

For all datasets, we usually observe higher AUC for PoS+ than its PoS variant suggesting the expressiveness power of center-common-neighbor pooling over simple center pooling. Of course, these slight AUC improvements come with slightly higher computational costs (see Table 3).

***S3GRL* as a scalability framework.** To demonstrate the flexibility of *S3GRL* as a scalability framework, we explore

	Model	Training	Preproc.	Runtime	AUC
Cora	PoS	4.82 ± 0.25	83.28 ± 3.16	336.70 ± 2.47	94.65 ± 0.67
	PoS + ScaLed	4.73 ± 0.22	60.32 ± 3.50	308.73 ± 4.27	94.35 ± 0.52
	PoS ⁺	5.59 ± 0.31	94.33 ± 7.36	387.95 ± 7.81	94.77 ± 0.65
	PoS ⁺ + ScaLed	5.49 ± 0.28	69.95 ± 5.12	358.40 ± 7.08	94.80 ± 0.58
CiteSeer	PoS	4.66 ± 0.20	61.86 ± 0.64	308.20 ± 2.86	95.76 ± 0.59
	PoS + ScaLed	4.65 ± 0.21	56.65 ± 2.59	302.45 ± 3.95	95.52 ± 0.65
	PoS ⁺	4.72 ± 0.35	79.14 ± 5.34	330.29 ± 5.61	95.60 ± 0.52
	PoS ⁺ + ScaLed	4.66 ± 0.27	65.56 ± 5.13	313.38 ± 6.25	95.60 ± 0.53

Table 4: Results for *S3GRL* as a scalability framework: ScaLed’s subgraph sampling combined with PoS and PoS⁺.

how easily it can host other scalable SGRLs. Specifically, we exchange the subgraph sampling strategy of PoS (and PoS⁺) with the random-walk induced subgraph sampling technique in ScaLed. We fixed its hyperparameters, the random walk length $h = 3$, and the number of random walks $k = 20$. Table 4 shows the average computational time and AUC (over 10 runs). The subgraph sampling of ScaLed offers further speedup in PoS and PoS⁺ in training, dataset preprocessing, and overall runtimes. For PoS⁺ variants, we even witness AUC gains on Cora and no AUC losses on CiteSeer. The AUC gains of PoS⁺ could be attributed to the regularization offered through sparser enclosing subgraphs. This demonstration suggests that *S3GRL* can provide a foundation for hosting various SGRLs to further boost their scalability.

7 Conclusions and Future Work

Subgraph representation learning methods (SGRLs), albeit comprising state-of-the-art models for link prediction, suffer from large computational overheads. In this paper, we propose a novel SGRL framework *S3GRL*, aimed at faster inference and training times while offering flexibility to emulate many other SGRLs. We achieve this speedup through easily precomputable subgraph-level diffusion operators in place of expensive message-passing schemes. *S3GRL* supports multiple subgraph selection choices for the creation of the operators, allowing for a multi-scale view around the target links. Our experiments on multiple instances of our *S3GRL* framework show significant computational speedup over existing SGRLs, while offering matching (or higher) link prediction efficacies. For future work, we intend to devise learnable subgraph selection and diffusion operators, that are catered to the training dataset and computational constraints.

References

- [Abu-El-Haija *et al.*, 2020] Sami Abu-El-Haija, Amol Kapoor, Bryan Perozzi, and Joonseok Lee. N-gcn: Multi-scale graph convolution for semi-supervised node classification. In *Uncertainty in Artificial Intelligence*, 2020.
- [Adamic and Adar, 2003] Lada A Adamic and Eytan Adar. Friends and neighbors on the web. *Social Networks*, 25(3):211–230, 2003.
- [Bruna *et al.*, 2014] Joan Bruna, Wojciech Zaremba, Arthur Szlam, and Yann Lecun. Spectral networks and locally connected networks on graphs. In *International Conference on Learning Representations*, 2014.
- [Cai and Ji, 2020] Lei Cai and Shuiwang Ji. A multi-scale approach for graph link prediction. In *AAAI Conference on Artificial Intelligence*, 2020.
- [Chamberlain *et al.*, 2022] Benjamin Paul Chamberlain, Sergey Shirobokov, Emanuele Rossi, Fabrizio Frasca, Thomas Markovich, Nils Hammerla, Michael M Bronstein, and Max Hansmire. Graph neural networks for link prediction with subgraph sketching. *arXiv preprint arXiv:2209.15486*, 2022.
- [Chen *et al.*, 2018] Jie Chen, Tengfei Ma, and Cao Xiao. FastGCN: Fast learning with graph convolutional networks via importance sampling. In *International Conference on Learning Representations*, 2018.
- [Chen *et al.*, 2020] Liang Chen, Yuanzhen Xie, Zibin Zheng, Huayou Zheng, and Jingdun Xie. Friend recommendation based on multi-social graph convolutional network. *IEEE Access*, 8:43618–43629, 2020.
- [Clevert *et al.*, 2015] Djork-Arné Clevert, Thomas Unterthiner, and Sepp Hochreiter. Fast and accurate deep network learning by exponential linear units (elus). *arXiv preprint arXiv:1511.07289*, 2015.
- [Davidson *et al.*, 2018] Tim R. Davidson, Luca Falorsi, Nicola De Cao, Thomas Kipf, and Jakub M. Tomczak. Hyperspherical variational auto-encoders. In *Uncertainty in Artificial Intelligence*, 2018.
- [Defferrard *et al.*, 2016] Michaël Defferrard, Xavier Bresson, and Pierre Vandergheynst. Convolutional neural networks on graphs with fast localized spectral filtering. In *Advances in Neural Information Processing Systems*, 2016.
- [Fey and Lenssen, 2019] Matthias Fey and Jan E. Lenssen. Fast graph representation learning with PyTorch Geometric. In *ICLR Workshop on Representation Learning on Graphs and Manifolds*, 2019.
- [Frasca *et al.*, 2020] Fabrizio Frasca, Emanuele Rossi, Davide Eynard, Benjamin Chamberlain, Michael Bronstein, and Federico Monti. Sign: Scalable inception graph neural networks. In *ICML 2020 Workshop on Graph Representation Learning and Beyond*, 2020.
- [Gasteiger *et al.*, 2019] Johannes Gasteiger, Stefan Weißenberger, and Stephan Günnemann. Diffusion improves graph learning. In *Advances in Neural Information Processing Systems*, 2019.
- [Granovetter, 1983] Mark Granovetter. The strength of weak ties: A network theory revisited. *Sociological theory*, pages 201–233, 1983.
- [Grover and Leskovec, 2016] Aditya Grover and Jure Leskovec. node2vec: Scalable feature learning for networks. In *International Conference on Knowledge Discovery and Data Mining*, 2016.
- [Guo *et al.*, 2022] Zhichun Guo, William Shiao, Shichang Zhang, Yozen Liu, Nitesh Chawla, Neil Shah, and Tong Zhao. Linkless link prediction via relational distillation. *arXiv preprint arXiv:2210.05801*, 2022.

- [Hamilton *et al.*, 2017] William L. Hamilton, Rex Ying, and Jure Leskovec. Inductive representation learning on large graphs. In *Advances in Neural Information Processing Systems*, 2017.
- [Hamilton, 2020] William L Hamilton. Graph representation learning. *Synthesis Lectures on Artificial Intelligence and Machine Learning*, 14(3):1–159, 2020.
- [Huang *et al.*, 2020] Kexin Huang, Cao Xiao, Lucas M Glass, Marinka Zitnik, and Jimeng Sun. Skipggn: predicting molecular interactions with skip-graph networks. *Scientific reports*, 10(1):1–16, 2020.
- [Huang *et al.*, 2022] Yinan Huang, Xingang Peng, Jianzhu Ma, and Muhan Zhang. Boosting the cycle counting power of graph neural networks with I^2 -gtns. *arXiv preprint arXiv:2210.13978*, 2022.
- [Katz, 1953] Leo Katz. A new status index derived from sociometric analysis. *Psychometrika*, 18(1):39–43, 1953.
- [Kingma and Ba, 2015] Diederik P. Kingma and Jimmy Ba. Adam: A method for stochastic optimization. In *International Conference on Learning Representations*, 2015.
- [Kipf and Welling, 2016] Thomas N Kipf and Max Welling. Variational graph auto-encoders. *arXiv preprint arXiv:1611.07308*, 2016.
- [Kipf and Welling, 2017] Thomas N. Kipf and Max Welling. Semi-supervised classification with graph convolutional networks. In *International Conference on Learning Representations*, 2017.
- [Koren *et al.*, 2009] Yehuda Koren, Robert Bell, and Chris Volinsky. Matrix factorization techniques for recommender systems. *Computer*, 42(8):30–37, 2009.
- [Li *et al.*, 2020] Pan Li, Yanbang Wang, Hongwei Wang, and Jure Leskovec. Distance encoding: Design provably more powerful neural networks for graph representation learning. In *Advances in Neural Information Processing Systems*, 2020.
- [Liben-Nowell and Kleinberg, 2003] David Liben-Nowell and Jon Kleinberg. The link prediction problem for social networks. In *International Conference on Information and Knowledge Management*, 2003.
- [Louis *et al.*, 2022] Paul Louis, Shweta Ann Jacob, and Amirali Salehi-Abari. Sampling enclosing subgraphs for link prediction. In *International Conference on Information & Knowledge Management*, 2022.
- [Mavromatis and Karypis, 2021] Costas Mavromatis and G. Karypis. Graph infoclust: Maximizing coarse-grain mutual information in graphs. In *PAKDD*, 2021.
- [Page *et al.*, 1999] Lawrence Page, Sergey Brin, Rajeev Motwani, and Terry Winograd. The pagerank citation ranking: Bringing order to the web. Technical report, Stanford InfoLab, 1999.
- [Pan *et al.*, 2018] Shirui Pan, Ruiqi Hu, Guodong Long, Jing Jiang, Lina Yao, and Chengqi Zhang. Adversarially regularized graph autoencoder for graph embedding. In *International Joint Conference on Artificial Intelligence*, 2018.
- [Pan *et al.*, 2022] Liming Pan, Cheng Shi, and Ivan Dokmanić. Neural link prediction with walk pooling. In *International Conference on Learning Representations*, 2022.
- [Paszke *et al.*, 2019] Adam Paszke, Sam Gross, Francisco Massa, Adam Lerer, James Bradbury, Gregory Chanan, Trevor Killeen, Zeming Lin, Natalia Gimelshein, Luca Antiga, Alban Desmaison, Andreas Köpf, Edward Yang, Zach DeVito, Martin Raison, Alykhan Tejani, Sasank Chilamkurthy, Benoit Steiner, Lu Fang, Junjie Bai, and Soumith Chintala. Pytorch: An imperative style, high-performance deep learning library. In *Advances in Neural Information Processing Systems*, 2019.
- [Perozzi *et al.*, 2014] Bryan Perozzi, Rami Al-Rfou, and Steven Skiena. Deepwalk: Online learning of social representations. In *International Conference on Knowledge Discovery and Data mining*, 2014.
- [Pho and Mantzaris, 2022] Patrick Pho and Alexander V. Mantzaris. Link prediction with simple graph convolution and regularized simple graph convolution. In *International Conference on Information System and Data Mining*, 2022.
- [Vaswani *et al.*, 2017] Ashish Vaswani, Noam Shazeer, Niki Parmar, Jakob Uszkoreit, Llion Jones, Aidan N. Gomez, Łukasz Kaiser, and Illia Polosukhin. Attention is all you need. In *Advances in Neural Information Processing Systems*, 2017.
- [Wu *et al.*, 2019] Felix Wu, Amauri Souza, Tianyi Zhang, Christopher Fifty, Tao Yu, and Kilian Weinberger. Simplifying graph convolutional networks. In *International Conference on Machine Learning*, 2019.
- [Xiong *et al.*, 2019] Zhaoping Xiong, Dingyan Wang, Xi-aohong Liu, Feisheng Zhong, Xiaozhe Wan, Xutong Li, Zhaojun Li, Xiaomin Luo, Kaixian Chen, Hualiang Jiang, et al. Pushing the boundaries of molecular representation for drug discovery with the graph attention mechanism. *Journal of medicinal chemistry*, 63(16):8749–8760, 2019.
- [Xu *et al.*, 2018] Keyulu Xu, Chengtao Li, Yonglong Tian, Tomohiro Sonobe, Ken-ichi Kawarabayashi, and Stefanie Jegelka. Representation learning on graphs with jumping knowledge networks. In *International Conference on Machine Learning*, 2018.
- [Yin *et al.*, 2022] Haoteng Yin, Muhan Zhang, Yanbang Wang, Jianguo Wang, and Pan Li. Algorithm and system co-design for efficient subgraph-based graph representation learning. *Proceedings of the VLDB Endowment*, 15(11):2788–2796, 2022.
- [Ying *et al.*, 2018] Rex Ying, Ruining He, Kaifeng Chen, Pong Eksombatchai, William L Hamilton, and Jure Leskovec. Graph convolutional neural networks for web-scale recommender systems. In *International Conference on Knowledge Discovery and Data mining*, 2018.
- [Zeng *et al.*, 2020] Hanqing Zeng, Hongkuan Zhou, Ajitesh Srivastava, Rajgopal Kannan, and Viktor Prasanna. GraphSAINT: Graph sampling based inductive learning method. In *International Conference on Learning Representations*, 2020.

- [Zeng *et al.*, 2021] Hanqing Zeng, Muhan Zhang, Yinglong Xia, Ajitesh Srivastava, Andrey Malevich, Rajgopal Kannan, Viktor Prasanna, Long Jin, and Ren Chen. Decoupling the depth and scope of graph neural networks. In *Advances in Neural Information Processing Systems*, 2021.
- [Zhang and Chen, 2017] Muhan Zhang and Yixin Chen. Weisfeiler-lehman neural machine for link prediction. In *International Conference on Knowledge Discovery and Data Mining*, 2017.
- [Zhang and Chen, 2018] Muhan Zhang and Yixin Chen. Link prediction based on graph neural networks. In *Advances in Neural Information Processing Systems*, 2018.
- [Zhang *et al.*, 2018] Muhan Zhang, Zhicheng Cui, Marion Neumann, and Yixin Chen. An end-to-end deep learning architecture for graph classification. In *AAAI Conference on Artificial Intelligence*, 2018.
- [Zhang *et al.*, 2020] Zhao Zhang, Fuzhen Zhuang, Hengshu Zhu, Zhiping Shi, Hui Xiong, and Qing He. Relational graph neural network with hierarchical attention for knowledge graph completion. In *AAAI Conference on Artificial Intelligence*, 2020.
- [Zhang *et al.*, 2021] Muhan Zhang, Pan Li, Yinglong Xia, Kai Wang, and Long Jin. Labeling trick: A theory of using graph neural networks for multi-node representation learning. In *Advances in Neural Information Processing Systems*, volume 34, 2021.
- [Zhong *et al.*, 2022] Wen Zhong, Changxiang He, Chen Xiao, Yuru Liu, Xiaofei Qin, and Zhensheng Yu. Long-distance dependency combined multi-hop graph neural networks for protein-protein interactions prediction. *BMC bioinformatics*, 23(1):1–21, 2022.
- [Zitnik *et al.*, 2018] Marinka Zitnik, Monica Agrawal, and Jure Leskovec. Modeling polypharmacy side effects with graph convolutional networks. *Bioinformatics*, 34(13):i457–i466, 2018.
- [Zou *et al.*, 2019] Difan Zou, Ziniu Hu, Yewen Wang, Song Jiang, Yizhou Sun, and Quanquan Gu. Layer-dependent importance sampling for training deep and large graph convolutional networks. In *Advances in Neural Information Processing Systems*, 2019.

A Additional Experimental Details

A.1 Hyperparameter Settings

For PPR, we set $\alpha = 0.85$. All methods (except heuristics, SGRL, and *S3GRL* methods) use a Hadamard product to create the link representation from the target pair’s representations. All autoencoder-based models use a GCN encoder to produce node embeddings and an inner product of the learned node embedding matrix to reconstruct the original adjacency matrix. The hidden dimensionality (i.e., dimensions of embeddings) for all baselines is set to 32 except for the autoencoder models, SEAL, and GCN+DE. Autoencoder models use varying-sized hidden dimensionalities, ranging from 32 to 64, for their encoders whereas SEAL and GCN+DE have 256 hidden dimensions for the attributed datasets.

We normalize the adjacency matrix of the selected subgraphs in PoS and PoS⁺ and the input graph adjacency matrix in SoP. Our graph normalization is symmetric degree normalization without additional self-loops. For *S3GRL* models trained on the non-attributed datasets, we use 16-dimensional node2vec pretrained embeddings [Grover and Leskovec, 2016] as the initial node features. In *S3GRL* models, we augment each subgraph’s initial feature matrix with the zero-one labeling scheme. Additionally, *S3GRL* models are implemented with a weight decay of 0.0001 and the ELU [Clevert *et al.*, 2015] activation function as the non-linearity function.

To fit the datasets into memory, we train SEAL and GCN+DE on Pubmed in a dynamic train mode (i.e., subgraphs are extracted on the fly during training), and we set the maximum number of nodes per hop to 100 for WalkPool on Ecoli, PB, and Pubmed datasets. For SEAL and WalkPool, we augment the initial node features with DRNL labeling whereas GCN+DE deploys a distance-encoding labeling scheme. For our baselines, the initial node features for non-attributed datasets are set to identity, except in WalkPool with a 16-dimensional vector of ones, and SEAL and GCN+DE with no node features. Finally, Walkpool, SEAL, and GCN+DE use a 32-dimensional embedding table for learning the node labels.

A.2 Datasets

All datasets used in our experiments are publicly available and have been subject to other link prediction studies [Zhang and Chen, 2018; Zhang *et al.*, 2018; Li *et al.*, 2020; Pan *et al.*, 2022; Louis *et al.*, 2022]. For the non-attributed datasets, we utilize the dataset files shared in [Zhang and Chen, 2018].⁹ For the attributed datasets we utilize Pytorch Geometric’s [Fey and Lenssen, 2019] dataset modules.¹⁰

A.3 Reproducibility

All our experiments are performed over fixed random seeds ensuring reproducibility if repeated multiple times on the same hardware.¹¹

⁹<https://github.com/muhanzhang/SEAL/tree/master/MATLAB/data>

¹⁰<https://pytorch-geometric.readthedocs.io/en/latest/modules/datasets.html>

¹¹Random numbers generated on different hardware could slightly vary our results. But, rerunning experiments on the same hardware ensures reproducibility on the same machine.